Characteristics of North American Summertime Rainfall with Emphasis on the Monsoon

BRANT LIEBMANN

Cooperative Institute for Research in Environmental Sciences, Climate Diagnostics Center, Boulder, Colorado

ILEANA BLADÉ

Departament d'Astronomia i Meteorologia, Facultat de Física, Universitat de Barcelona, Barcelona, Spain

NICHOLAS A. BOND

University of Washington, and Joint Institute for the Study of the Atmosphere and Ocean, Seattle, Washington

DAVID GOCHIS

Research Applications Laboratory, National Center for Atmospheric Research, Boulder, Colorado

DAVE ALLURED AND GARY T. BATES

Cooperative Institute for Research in Environmental Sciences, Climate Diagnostics Center, Boulder, Colorado

(Manuscript received 7 November 2006, in final form 17 May 2007)

ABSTRACT

The core region of the North American summer monsoon is examined using spatially averaged daily rainfall observations obtained from gauges, with the objective of improving understanding of its climatology and variability. At most grid points, composite and interannual variations of the onset and end of the wet season are well defined, although, among individual stations that make up a grid average, variability is large. The trigger for monsoon onset in southern and eastern Mexico appears to be related to a change in vertical velocity, while for northwestern Mexico, Arizona, and New Mexico it is related to a reduction in stability, as indicated by a decrease in the lifted index. The wet-season rain rate is a combination of the wet-day rain rate, which decreases with distance from the coast, and the wet-day frequency, which is largest over the Sierra Madre Occidental. Thus the maximum total rate lies slightly to the west of the highest orography. As has been previously noted, onset is not always well correlated with total seasonal precipitation, so in these areas, variations of wet-day frequency and wet-day rain rate must be important. Correlations are small between the wet-day frequency and the wet-day rate, and the former is better correlated than the latter with the seasonal rain rate. Summer rainfall in central to southern Mexico exhibits moderate negative correlations with the leading pattern of sea surface temperature (SST) anomalies in the equatorial Pacific, which projects strongly onto El Niño. The influence of equatorial SSTs on southern Mexico rainfall seems to operate mainly through variability of the wet-day frequency, rather than through variations of the wet-day rain rate.

1. Introduction

The North American monsoon (NAM) system extends from the intertropical convergence zone of the eastern Pacific Ocean to the Bermuda high, and from Central America to Canada (Ropelewski et al. 2005; Mechoso et al. 2005). Modulations in the magnitude and extent of the large-scale NAM circulation influence, in part, the mechanisms (e.g., the Gulf of California low-level jet) responsible for the transport of moist tropical air into southwestern North America that, in turn, drive rainfall patterns that characterize monsoon behavior (e.g., Higgins et al. 1999, hereafter HCD99; Vera et al. 2006).

Corresponding author address: Brant Liebmann, NOAA/ESRL PSD Climate Diagnostics, R/PSD1, 325 Broadway, Boulder, CO 80305-3328.
E-mail: brant.liebmann@noaa.gov

DOI: 10.1175/2007JCLI1762.1

© 2008 American Meteorological Society

Rainfall associated with the monsoon accounts for a large fraction of the annual total precipitation over a large area centered in northwest Mexico (e.g., Douglas et al. 1993). In this central region, more than 70% of annual precipitation occurs during summer. In the United States, the direct influence of the monsoon is largest in New Mexico and Arizona, where more than 40% and 25% of annual precipitation, respectively, is received during summer (Douglas et al. 1993; Higgins et al. 1997, 1998; Ropelewski et al. 2005; Adams and Comrie 1997; HCD99). In other areas (e.g., the Front Range of Colorado), the monsoon is of lesser importance to the annual hydrological budget, but monsoon-related events, such as severe thunderstorm activity and flash flooding, make it still relevant for forecasting and hazard prevention.

The core of the monsoon, which is the subject of the present study, may also affect other areas indirectly, most notably the central United States. Several studies have shown (e.g., Douglas and Englehart 1996; Higgins et al. 1997; Barlow et al. 1998; HCD99) that during years with a strong monsoon in the southwestern United States, summer precipitation in the Great Plains and/or the southern central United States is reduced, and vice-versa. The mechanism for rain suppression over the plains when the monsoon is active appears to be forced subsidence east of the heating (Barlow et al. 1998), consistent with the development of upper-level convergence, which inhibits low-level-jet-related rainfall (Higgins et al. 1997).

Although there is some evidence of coherent variations across the entire monsoon core (e.g., Yu and Wallace 2000), interannual variability in the northern and southern part of the domain appears to be controlled by different mechanisms and to be associated with widely different circulation anomalies, with the separation between domains lying at about 26°N, across northern Mexico (Hu and Feng 2002). In the northern region (which includes the southwestern United States), years of abundant monsoon rainfall are characterized by an upper-level ridge that is displaced northward of its mean summer position; that is, the monsoon anticyclone is enhanced (e.g., Carleton et al. 1990; Adams and Comrie 1997; HCD99), which increases midlevel moisture transport from the Gulf of Mexico (e.g., Castro et al. 2001). On the other hand, wet years in the southern Mexico domain are characterized by an upper-level trough over the southwest United States and a retracted North Pacific jet, reminiscent of the circulation anomalies observed during La Niña (HCD99). The situations are approximately opposite during dry years.

Consistent with the above differences, the northern and southern core monsoon regions exhibit widely different relationships with tropical Pacific SSTs and the Southern Oscillation index (SOI). In the south, monsoon rainfall and streamflow are modestly correlated with the SOI, with a sign suggesting that El Niño events are associated with a seasonal deficit in rainfall (HCD99; Gochis et al. 2007a). The corresponding increase in precipitation during La Niña has been attributed to the northward displacement of the eastern Pacific intertropical convergence zone (ITCZ), which results in increased northward transport of water vapor (Hu and Feng 2002), as well as to cool SSTs off the southern Mexican coast, which increases the land–sea thermal contrast (HCD99).

In contrast to their impact over southern Mexico, equatorial Pacific SSTs have only a small and inconsistent influence on monsoon rainfall in the northern part of the domain. For instance, by defining indices of June–September precipitation for Arizona–New Mexico and northwest Mexico separately, and computing composite changes during ENSO years, HCD99 found changes of less than +1% and −10.3%, respectively, during El Niño, and −8.5% and −2.2% during La Niña. Castro et al. (2001), however, concluded that the concurrence of El Niño with the positive phase of the North Pacific Oscillation (NPO)—warm eastern North Pacific and cool central North Pacific—favors dry monsoon conditions in the southwestern United States, while wet conditions are favored when the negative phase of the NPO coincides with a La Niña event. There are also suggestions that, in this northern monsoon domain, antecedent winter precipitation may play a role in modulating summer precipitation (e.g., Gutzler 2000; Hu and Feng 2002), with winters with increased snowpack in the western United States preceding summers with decreased summer precipitation. This relationship, however, is not consistent over the period of record (Gutzler 2000; Higgins and Shi 2000; Hu and Feng 2002, 2004).

The differences between the northern and southern domains may extend to the dynamics of onset. In the northern monsoon region, onset of the wet season is characterized by a northward shift of the upper-level climatological subtropical ridge and establishment of deep easterlies over most of Mexico (Douglas et al. 1993) with southwesterly flow over the southwestern United States (Higgins et al. 1997). In contrast, the circulation and moisture fluxes associated with onset in southern Mexico have received comparatively little attention. The actual triggering mechanisms—that is, whether changes in static stability or in vertical velocity play a determinant role in initiating the convection—are even less well understood.

Likewise, while many studies have explored possible causes for year-to-year variations in the North American monsoon, fewer document the internal characteristics of these variations. Interannual variability of summertime monsoon precipitation results from variations in quantities such as the length of the wet season and its intensity (Englehart and Douglas 2006). They found that in northwest Mexico (Sonora) that a trend of decreasing wet season length is largely compensated for by increasing intensity. HCD99 and Higgins and Shi (2000) found that the date of onset in Arizona–New Mexico (AZNM) is moderately correlated (~0.5) with June–September rainfall, with the expected sign of an early onset leading to increased seasonal rainfall. Higgins and Shi (2000) also found a correlation of 0.67 between an index of winter North Pacific SSTs and AZNM onset, so cold SSTs in the midlatitude central North Pacific precede an early monsoon onset. Thus the modulation of total monsoon rainfall in this region by fluctuations in North Pacific SSTs appears to be due, at least partly, to the influence of those SST anomalies on the timing of onset.

On the other hand, the relationship between onset and total summer monsoon precipitation is not significant in northwest Mexico and is completely absent in southern Mexico (HCD99)—though in that region there is also relatively little year-to-year variation in the onset date. For northwest Mexico, Barlow et al. (1998) found a large increase in convective available potential energy (CAPE) around onset; they argued that this buildup of CAPE must be controlled by an increase in low-level moisture, as there is little concomitant change in surface temperature. Barlow et al. also found that, in this region, convective inhibition energy (CINE) exhibited little June to July change and was therefore of no relevance to onset. They suggested a dynamic influence on vertical velocity triggered by strong heating in regions of orography. These onset-related changes, however, were identified using July minus June differences, which represent a crude measure of onset that ignores large spatial and temporal variations.

All in all, it is clear that a good understanding of the processes that initiate deep convection in the various sectors of the monsoon is presently lacking. Little additional insight can be gained from model simulations since most GCMs tend to delay onset relative to observations (Gutzler et al. 2005). In addition to its scientific interest, a better physical understanding of onset dynamics in nature is of particular practical importance since it could guide model developments to improve the representation of onset in GCMs, which could in turn lead to skillful seasonal predictions of monsoon rainfall. From the studies cited above it is also apparent that variability of total seasonal precipitation within the North American monsoon system is not dominated by variations in a single quantity. Onset variations seem to be important in the north, while within-season variations must dominate in the south. In areas in which onset does not modulate the seasonal precipitation total, variations in the wet-season rain rate must account for interannual variations in that seasonal total, provided variations in the end date are minimal. Likewise, if such areas exhibit strong relationships between SSTs and seasonal total rainfall, the SST influence must operate through changes in the wet-season rain rate.

This paper improves on past studies of the NAM by using a more complete, high-resolution, precipitation dataset that covers the entire Mexican as well as U.S. domains, and by using a very precise definition of onset for each location and year. It presents a refined analysis of the climatology and interannual variability of various aspects of the NAM, in particular a detailed examination of quantities that may play a role a role in the initiation of the monsoon in the various monsoon domains, specifically the lifted index and vertical velocity. We also investigate the climatology and variability of precipitation characteristics that account for the year-to-year variations in total seasonal rainfall, such as wet season length and rate, wet-day rate, and frequency. Finally, we assess the role of interannual fluctuations of tropical Pacific SST in modulating all of the above quantities. Note that, while tropical storms are important to the overall climatology of warm season precipitation in western Mexico (e.g., Englehart and Douglas 2001), the present work does not explicitly distinguish the role of landfalling tropical storms in modulating precipitation statistics.

2. Data

Daily station rainfall records from U.S. and Mexican sources are the primary data used in this study (see acknowledgments). Of particular relevance to this study are stations from Mexico, within which lies the heart of the monsoon (Douglas et al. 1993). The Mexican dataset includes more than 5000 daily station records with an average record length of 22.3 yr for the period 1966 to 2000. This study period was chosen because there are at least 2400 Mexican records for each of those years (except for 1999 for which there are only 2275 records). An average of 7.6% of daily observations are missing in years with data.

Daily grids at 1° resolution are calculated by averaging all nonduplicate stations within a radius of 0.75° of the gridpoint center. Details of the gridding algorithm and the quality control procedures are almost identical

to those used by Liebmann and Allured (2005) to construct gridded precipitation data for South America. When and where they occur, missing data are simply ignored. The assumption, which has been validated in previous studies (e.g., Liebmann et al. 2004), is that, since the gridded value is an average of many stations, occasional missing observations cause fewer problems than if all incomplete stations were excluded. Similarly, it is assumed that data quality issues related to erroneous reporting of precipitation (e.g., zero precipitation versus "no data" or multiday accumulations reported on a single day) do not exhibit any particular spatial coherence and thus do not systematically impact the diagnosis of continental-scale patterns of precipitation characteristics reported here. One attribute of the dataset used here is that the station density is approximately the same in the United States and Mexico. This is important as previous studies with fewer Mexican stations have found a suspicious lack of cross-border coherence (e.g., Gutzler 2004).

Daily maximum and minimum temperature records (see acknowledgments) are also averaged onto grids at the same resolution (with little quality control). In Mexico, the temperature station density is approximately the same as that of the rain gauge network.

Other fields used in this study include 500-mb vertical velocity (omega), the lifted index (LI), and sea surface temperatures (SSTs). Daily omega and LI data are from the North American Regional Reanalysis (NARR; Mesinger et al. 2006); monthly SST fields are from the National Centers for Environmental Prediction–National Center for Atmospheric Research reanalysis (Kalnay et al. 1996). The NARR is available from 1979 only.

3. Results

a. Climatology

1) ONSET CHARACTERISTICS AND DYNAMICS

Figure 1 shows the annual total precipitation climatology. Parts of southern Mexico receive more than 2 m per year, but the majority of the country receives less than a meter. The driest area lies in the northwest of the domain, with totals of less than 0.2 m per year extending into the California–Arizona border area. An elongated area whose axis roughly parallels the Sierra Madre Occidental receives somewhat more precipitation than do regions to the east or west. This area is more-or-less coincident with the heart of the North American monsoon, which was identified by Douglas et al. (1993) as the region having a pronounced rainfall maximum during summer.

The blank grid cell located along the U.S.–Mexican border in southern Texas results from a lack of stations there. In subsequent maps, the value at this point will be calculated as the average of the value at the four nearest grid points in order to improve the maps' visual appeal. This is the only grid point onto which data have been interpolated.

Monthly climatologies and measures of interannual monthly variability for selected grid points within and surrounding the monsoon region are also shown in Fig. 1. The locations that are roughly aligned with the axis of the monsoon all show a distinct summer maximum, with relatively small interannual variability of monthly totals (sites b and c). Farther north, in Arizona (site a), precipitation also peaks during summer, although the peak occurs one month later than in the monsoon core and it is accompanied by an equally important peak in late winter/early spring. The interannual variability there is also relatively large. Farther to the west, at that same latitude, summer precipitation diminishes, while that during winter increases (not shown). The point in New Mexico (site i) has a single summer maximum with a modest standard deviation. Central Mexico, east of the monsoon (sites d and e), has a single summer peak, but the interannual variability is relatively large.

Southern Mexico (sites f and g), with an overall precipitation maximum during summer, exhibits a relative minimum in July and August. This signal is part of a "midsummer drought" (Portig 1961) that extends from southern Mexico into Central America and may be associated with fluctuations in the intensity and position of the eastern Pacific ITCZ (Magaña et al. 1999). These authors have argued that convection in the ITCZ experiences a midsummer minimum itself, as a result of which the trade winds intensify over the Caribbean. These circulation changes favor precipitation on the eastern side of the Central American orographic barrier and inhibit it on the western side. Alternatively, Mapes et al. (2005) have suggested an explanation in terms of a disequilibrium within the land–atmosphere system. The midsummer minimum and September maximum farther to the north, along the Gulf of Mexico (site h), may result instead from an increase in late-summer tropical disturbances.

Year-to-year variations in total wet season rainfall are determined by variations in the wet-season rain rate and length. Obviously, a correct estimate of all these quantities depends on an accurate identification of wet season onset and end. Additionally, if calendar season totals are of interest, then understanding variations in the timing of the wet season (i.e., its beginning and end) may also be important (provided these occur within the season of interest).

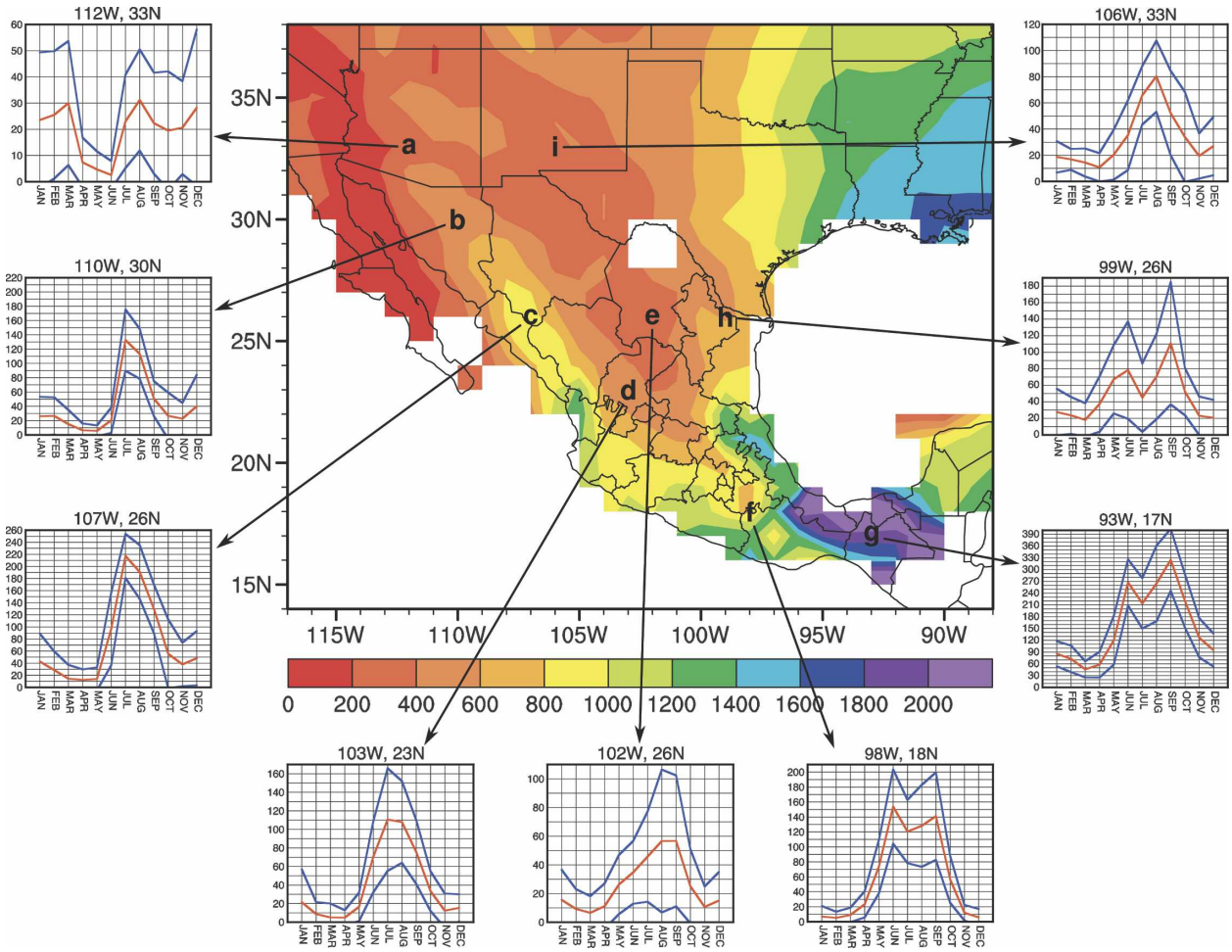

FIG. 1. Climatological annual total precipitation for the period 1966–2000 (mm). Plotted at the perimeter are monthly climatologies for selected grid points. Red curves indicate climatological-mean monthly totals (mm). Blue curves indicate climatology ± 1 std dev. On all graphs, horizontal lines are plotted at 10-mm intervals.

To construct an algorithm to determine onset and end of the monsoon season, we first define a quantity denoted "anomalous accumulation" at each grid point:

$$A(\text{day}) = \sum_{n=1}^{\text{day}} (R(n) - \overline{R}), \qquad (1)$$

where $R(n)$ is the daily precipitation and $\overline{R}$ is the annually averaged daily precipitation (climatological annual total divided by 365). For the present study the summation is started 10 days prior to the beginning of the climatologically driest month, unless that month falls between July and January in which case the summation is started on 1 January of each year. This allows the algorithm to identify a summertime monsoon starting date at locations at which there are both summertime and wintertime wet seasons. This expression produces curves for each year at each grid point (provided there are no missing data).

Examples of anomalous accumulation curves are shown in Fig. 2a. Although no single year's curve can be described as "typical," a representative example is provided by the curve for grid point 32°N, 109°W centered slightly north of the Arizona–New Mexico–Mexico intersection, for year 1969 (dashed–dotted curve). The nearly straight downward curve from the beginning of the calculation until Julian day 188 (7 July) represents an extended dry period, as for each day the annual-mean daily climatological value is subtracted from that day's rainfall and that anomalous quantity is then added to the running sum. Some rainfall interrupts the downward slope around day 125 (5 May), which causes the curve to briefly turn upward. On day 189 (8 July) the wet season begins in earnest, as from that day forward rainfall exceeds its climatological value and the curve rises.

In the algorithm used, the onset of the wet season is

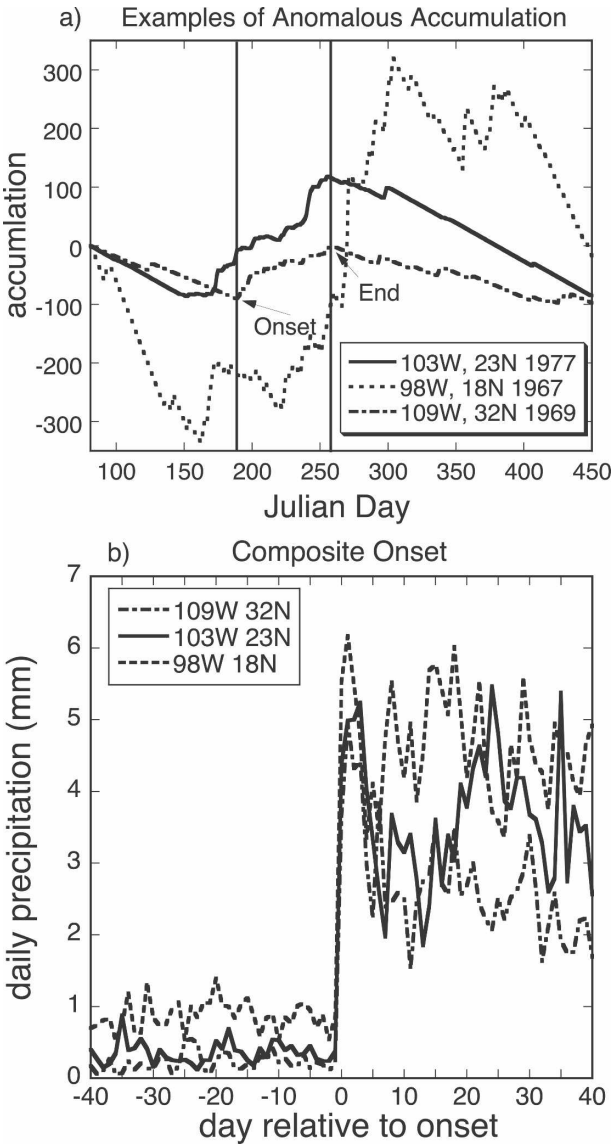

FIG. 2. (a) Examples of "anomalous accumulation" for grid points in southern Mexico (dotted curve), northwest Mexico (solid curve), and southwestern United States (dashed–dotted curve). See text for definition. Thick vertical lines represent date of onset and end of wet season for year 1969 at grid point 32°N, 109°W. (b) Composite rainfall about onset at same grid points.

defined as the beginning date of the longest period for which anomalous accumulation relative to that initial value is positive—provided this period occurs between the starting date of the summation and 27 October. This constraint ensures that the start of the winter-regime precipitation will never be interpreted as monsoon onset.

Near the core of the monsoon, represented here by the point at 23°N, 103°W (Fig. 2a, solid curve), this particular year (1977) is marked by an unusually slow transition between a long rainless period, which ends on 1 June (Julian day 152), and the wet season, which begins on 20 June (day 171). In this case, the algorithm chooses 1 June as the date of onset because anomalous accumulation is at an absolute minimum on 31 May. Although this example is unusual, it does illustrate the ambiguity of the onset date in years when onset is not abrupt.

The curve for southern Mexico (dotted curve) corresponds to an anomalously dry wet season, and was chosen because its vertical scale is similar to that of the other grid points. In most years the southern Mexico curve would be off the scale compared to curves at the other locations, owing to the abundant rainfall there (see Fig. 1). For this grid point and year, onset occurs on 9 June (day 160). It should be noted, however, that one cannot directly compare rainfall accumulations at different locations, as the climatology, which is subtracted from each day's total, is different at each point.

In areas dominated by the monsoon, ambiguities in determining onset date are relatively rare, which gives some confidence in the accuracy of the determined dates. Figure 2b shows the composite evolution of rainfall, relative to onset, for the entire 1966–2000 period at the same points as in Fig. 2a. A striking aspect of this figure is that, even after averaging over 35 yr, the evolution of rainfall is still quite noisy. It is also clear, however, that in a composite sense onset is captured reasonably well.

Each composite curve has a clear overshoot; that is, the accumulation amount at onset and for the first few days after onset is larger than the average for the subsequent several weeks. Higgins et al. (1997) composited precipitation about onset for an Arizona–New Mexico time series, using a threshold definition (0.5 mm for three consecutive days), and obtained a similar overshoot. They attributed the overshoot to the systematic occurrence of synoptic, as well as climate, events keyed to onset. An examination of the time series for individual years at 23°N, 103°W (Fig. 3a) shows large, seemingly random, variability after the initial onset event, reducing the post-onset average precipitation relative to the coherent precipitation at onset.

Shown in Fig. 3b are accumulation time series for some of the individual stations that compose the grid point at 23°N, 103°W, as well as the gridpoint average, for year 1996, plotted relative to gridpoint onset. The variability of precipitation among these stations is tremendous: for any given day of the period around onset, including onset day itself, some stations within the grid cell have no precipitation. As a general rule (from examination of many grid points and years), precipitation

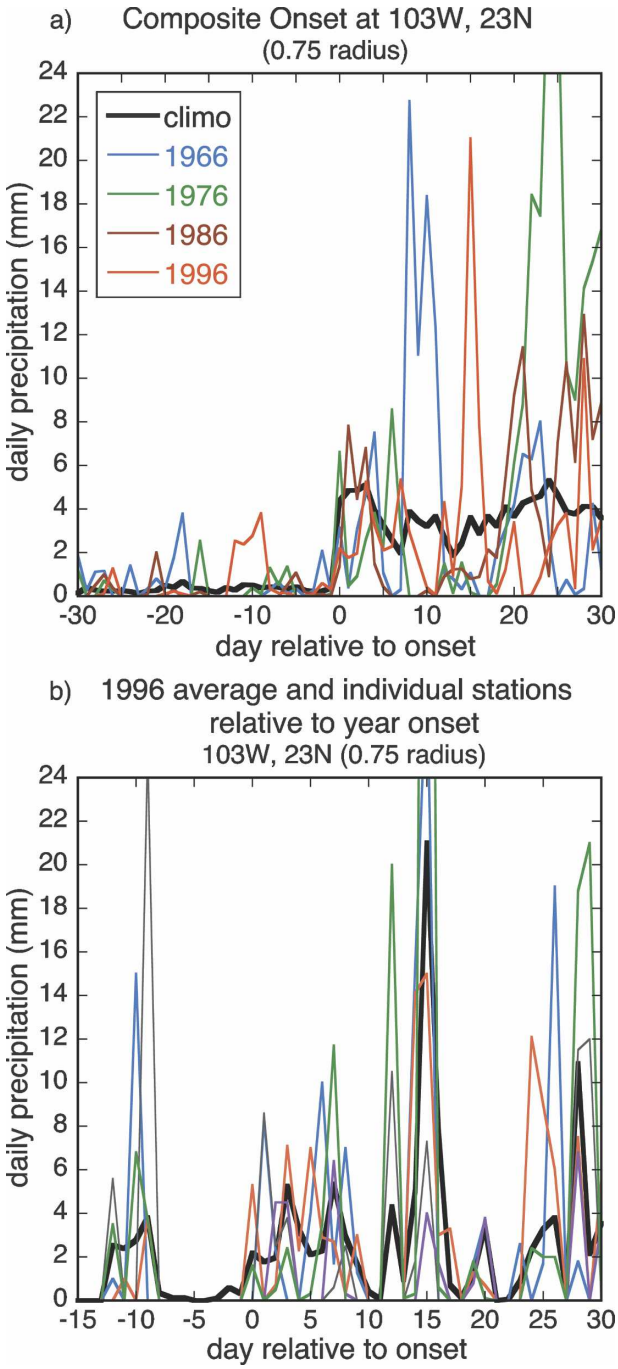

FIG. 3. (a) Composite onset (heavy curve) and onset for selected years at grid point located at 23°N, 103°W. (b) Onset at same grid point for year 1996 (heavy curve) and time series for selected stations included in gridpoint average.

rarely occurs simultaneously at all stations within a grid cell. While there appears to be a relatively slowly varying temporal modulation of the average precipitation, it is clear that this envelope is revealed only through temporally and spatially averaging.

Figure 4a shows the average onset date of the wet season. Away from the low-lying plains of the United States, the earliest starting dates are found in the area of the highest peaks in Mexico, at about 19°N, and near the eastern edge of the Mexican Plateau over the Sierra Madre Oriental at about 24°N, where onset occurs around the second week of May. By 12 June, the wet season is underway in most of southern and eastern Mexico. There is then a northwestward progression of onset dates, roughly along the axis of the monsoon, such that by 3 July the wet season is ongoing over most of Mexico. Onset in western New Mexico occurs right around that time, earlier than in Arizona. The gradient of onset dates becomes sharper in northern New Mexico and Colorado—a reflection of the abrupt transition between the springtime wet-season regime east of the Rockies and the summertime monsoon regime to the west. It should be noted, however, that the spring wet season over the Front Range of the Rocky Mountains and the Great Plains should not be considered as monsoon precipitation. This description of the progression of onset is roughly consistent with those of Douglas et al. (1993) and Douglas and Englehart (1996) and, over the core of the monsoon, with that of HCD99. Both these early descriptions, however, are based on a shorter period of record and lower grid resolution than in the present study. Some differences are also apparent. For example, in central Mexico, Fig. 4a shows onset to progress toward the coast, while the depiction in HCD99 (their Fig. 12) shows no such gradient. Note that this figure may give the misleading impression of a smooth progression of onset when, in fact, this is not the case. Indeed, HCD99 showed that correlations between onset dates in different regions are quite weak. On the other hand, Englehart and Douglas (2006) found a correlation of 0.51 between onset in northwest Mexico and Arizona.

The ending date is determined from the same anomalous accumulation curves used to define onset. It is defined as the day with the largest value after onset because, from that date onward, the accumulated rainfall (relative to that maximum value) is less than expected from the annual daily climatology. The caveat is that the end date must occur before 28 October; otherwise, at some locations (especially those under the influence of midlatitude storms) an early winter wet season could cause an upward spike in the anomalous accumulation curve that would not be physically related to the summertime precipitation regime. This end range for end dates was chosen after examination of accumulation curves for many years and many grid points: there almost always seems to be a break at around this time between summer and winter rainfall. While there are

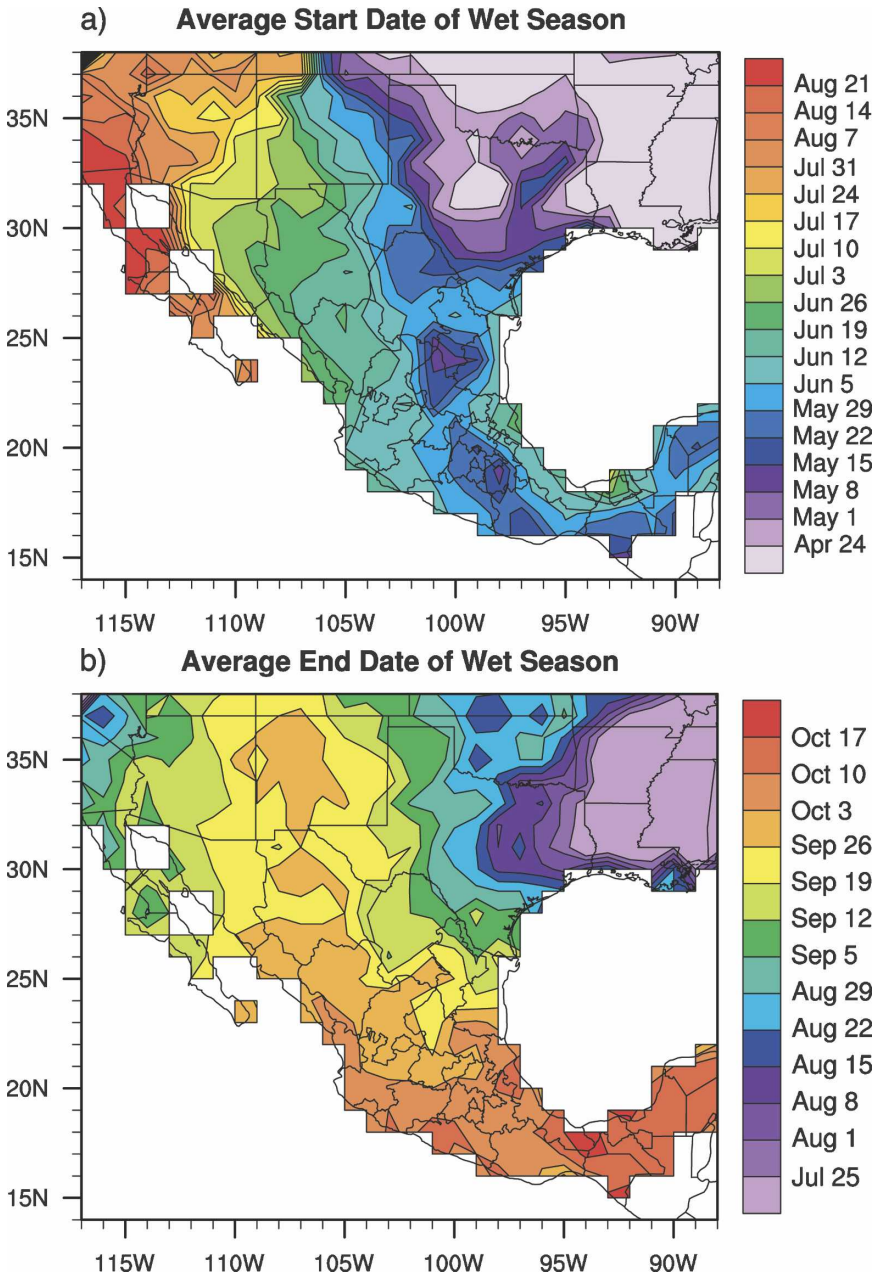

FIG. 4. (a) Start date at each grid point averaged from onset for each year; (b) as in (a), but for end date.

undoubtedly errors at some grid points that could be rectified by individual examination, in practice the general constraint seems to work well.

Figure 4b shows the average ending date. As expected, the wet season contracts toward the south, although it lingers until the end of September in mountainous western New Mexico. The end occurs rapidly along the spine of the monsoon; by about 1 October, within two weeks of its termination at the U.S.–Mexican border, the monsoon is contained almost entirely south of 20°N. The late ending near the Guatemala border is likely due to the presence of easterly waves in late summer, which may also account for the double climatological peak observed in that region (Fig. 1).

Composite differences of the maximum temperatures before and after wet season onset are presented in Fig. 5. Composite onset is always accompanied by a

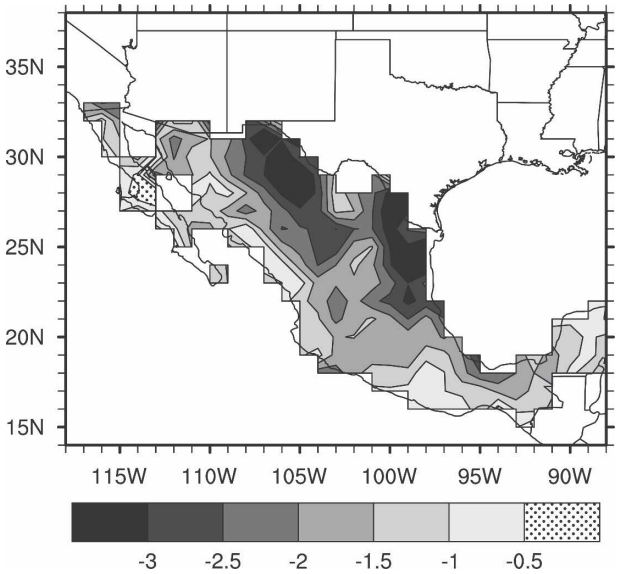

FIG. 5. Composite of daily maximum temperature (°C) averaged for two days after minus average for two days before onset at each grid point for the period 1966–2000.

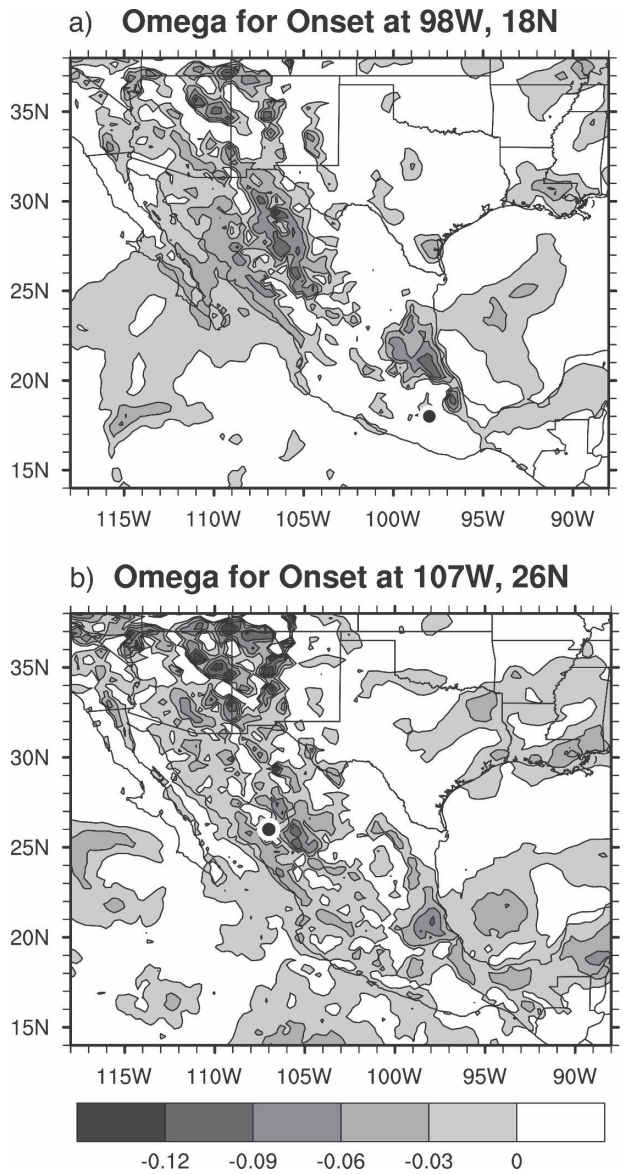

FIG. 6. (a) Composite 500-mb omega (mb s^{-1}) relative to day of onset (22 May) at grid point 18°N, 98°W indicated by the dot. (b) As in (a), but for day of onset (20 Jun) at grid point 26°N, 107°W. Omega fields are from the North American Regional Reanalysis. Averaging period is 1979–2000.

decrease in the maximum temperature. The uncertainty in the composite, however, is rather large: over the majority of Mexico, the interannual standard deviation of the difference is 60%–100% of the mean decrease and is even larger in other areas, especially in northwest Mexico. Corresponding composite changes in the minimum temperature are small (but with a large standard deviation), as are changes in the maximum and minimum temperature about the end of the wet season (not shown).

The temperature changes at the time of onset appear to reflect a response to rather than a cause of the development of sustained precipitation over Mexico. If an increase in surface temperature were responsible for the destabilization of the environment, a reduction following onset (as indicated by Fig. 5) should inhibit rainfall. Figure 5 would therefore suggest a surface temperature control on instability since precipitation does decrease after the initial spike (e.g., Fig. 2b). Time series of temperature evolution at selected grid points, however, indicate that, while the maximum temperature remains nearly steady prior to onset, it continues to gradually decrease after the initial sharp decrease at onset (not shown), which argues against the previous hypothesis. This result motivates the examination of other parameters more directly related to the propensity for deep convection. For simplicity, we focus here on two variables: the 500-mb omega velocity, an index of the dynamical forcing, and the LI, a measure of the static stability/thermodynamic control on deep convection (a *negative* LI indicates the possibility of convection). Both fields are derived from the NARR for the period 1979–2000. Our interest is in how these two parameters vary over the domain of interest.

The climatological-mean distributions of 500-mb omega and LI at the time of onset for a point in south-central Mexico (18°N, 98°W) and a point in northwestern Mexico (26°N, 107°W) are shown in Figs. 6 and 7. Both distributions feature significant northwest–southeast contrasts. The climatological 500-mb omega

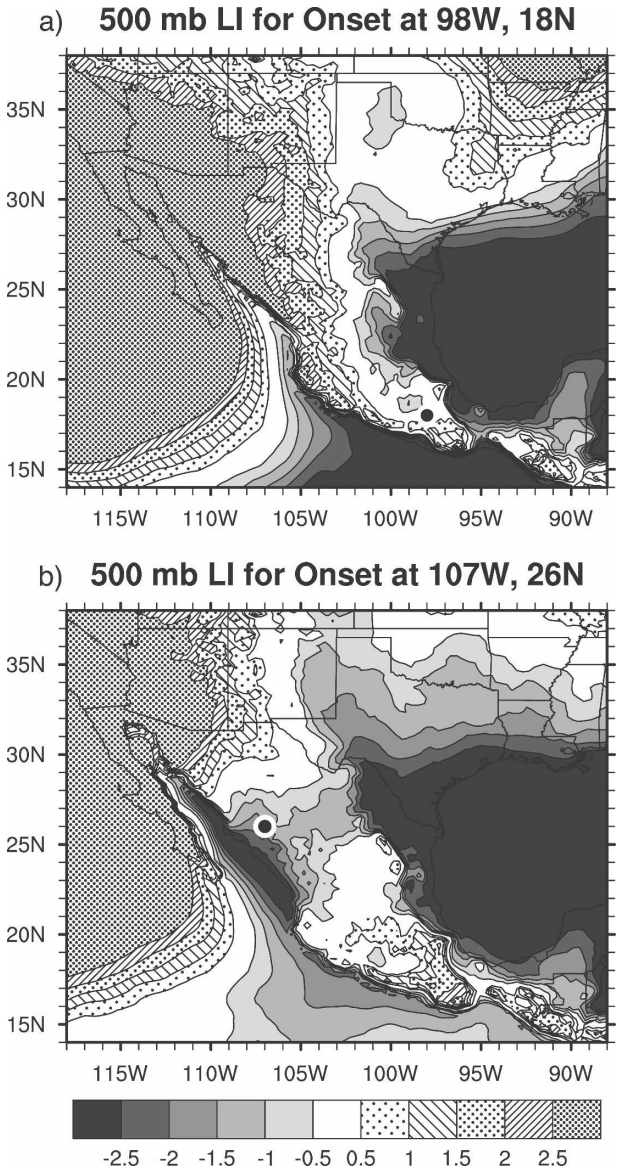

FIG. 7. As in Fig. 6, but for the lifted index (K). Lifted index fields are derived from the North American Regional Reanalysis.

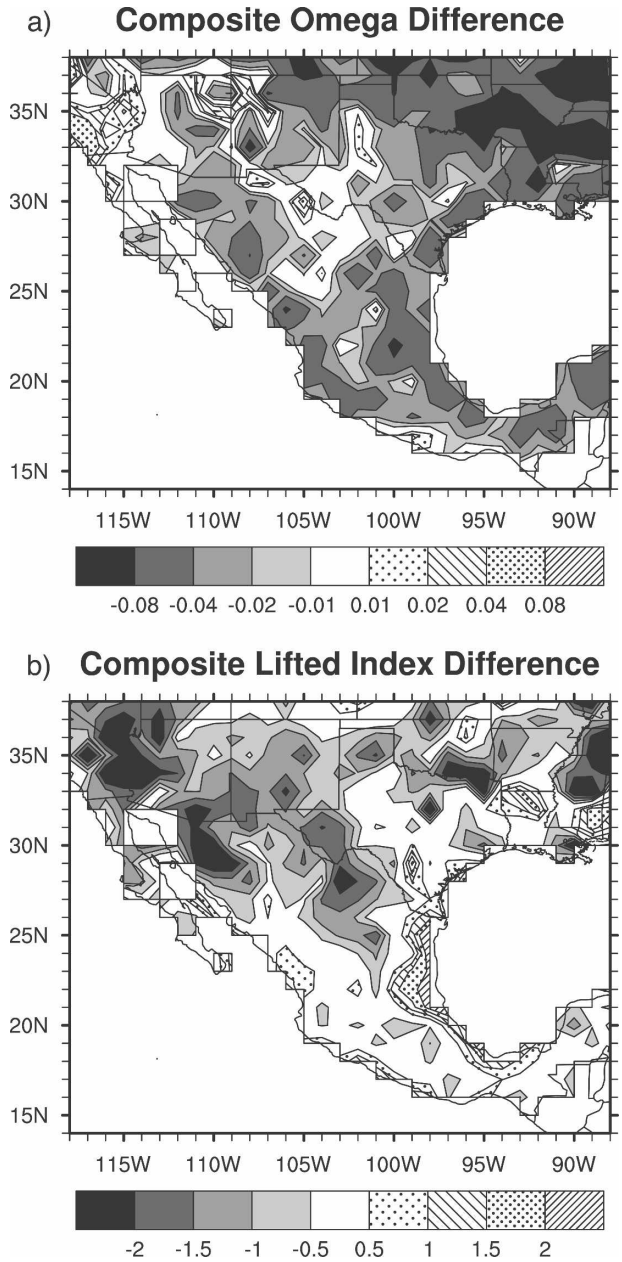

FIG. 8. (a) Point-by-point composite of the change in the anomalous 500-mb omega following onset, i.e., the average of days 2–4 after onset minus the average of days 2–4 before onset. Anomalies are computed relative to the daily climatology; units: mb s^{-1}. (b) As in (a), but for lifted index anomalies (K). Fields are regridded to match precipitation grid.

around 22 May (Fig. 6a), the time of year typically marking onset in south-central Mexico, indicates weak downward motion over most of southern Mexico but strong upward motion over northern Mexico, even though the wet season has not ordinarily commenced there. Its counterpart (Fig. 6b), the climatological 500-mb omega at the time of onset in northwest Mexico (around 20 June), indicates weak upward motion over northwestern Mexico and stronger upward motion over southern Mexico. In other words, the regional midtropospheric vertical velocity field is more favorable for deep convection *a month after* onset in southern Mexico, but *a month before* onset in northwestern Mexico, implying that upward motion is not a sufficient condition for development of deep convection in northwestern Mexico.

The most striking aspect of the mean LI distribution at the time of onset is the contrast between the extremely stable environment over the eastern Pacific at latitudes of Baja California and to the north and the

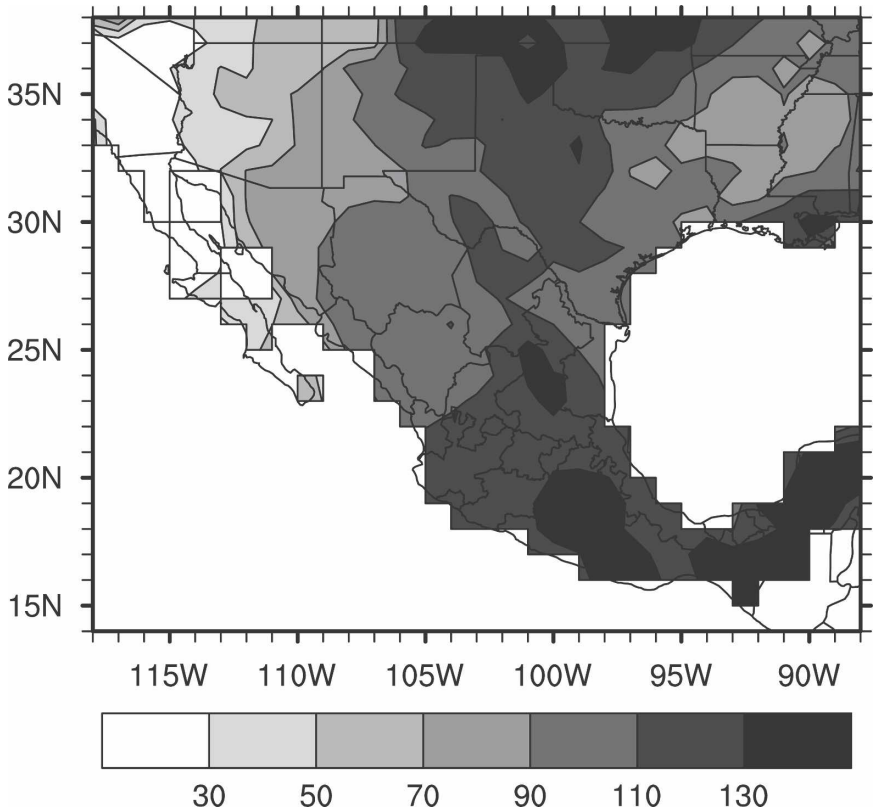

FIG. 9. Average wet season length (days).

large negative values in the Gulf of Mexico. Low values are also found in the eastern Pacific along the southern Mexican coast. The LI at onset in south-central Mexico (Fig. 7a) exhibits generally weakly negative (statically unstable) values in central southern Mexico and large positive (statically stable) values in northwestern Mexico. The pattern suggests that onset at the reference point might be occurring at the leading edge of a surge of unstable air from the Gulf of Mexico. At the time of onset in northwest Mexico (Fig. 7b), the LI values have changed little in southern and eastern Mexico. They have decreased markedly, however, in the vicinity of the reference point and over northern Mexico in general. Our interpretation of these results is that it is primarily the change in vertical velocity that is responsible for the development of wet conditions in southern Mexico since in that region the static stability is low from spring through summer, whereas it is destabilization that triggers the onset of precipitation in northwest Mexico since the midlevel vertical velocity is persistently upward prior to onset.

Additional support for this idea is provided by maps showing the composite differences in the mean 500-mb omega and LI fields 2–4 days before and after onset (Figs. 8a,b). These composites are local; that is, the difference is computed at each grid point relative to onset at that point. (For these calculations the NARR data was regridded to match the $1^\circ \times 1^\circ$ grid of observed precipitation.) The change in omega about onset is generally negative throughout the monsoon domain, but tends to be more pronounced in southern Mexico than in northwest Mexico and the southwestern United States. In contrast, the decrease in the LI is markedly stronger in the southwestern United States and northwestern Mexico than in southern Mexico. In fact, along the Mexican gulf coast and the southern Pacific coast, the LI change at onset is positive. These findings imply that the trigger for onset in southern and eastern Mexico is mainly related to a favorable change in vertical velocity, while for northwestern Mexico (and Arizona and New Mexico) it is more related to a reduction in LI. This result is consistent with forecast practices in the southwest United States, which key on low-level humidity (related to the LI) to characterize the beginning of the monsoon season.

2) WET-SEASON PRECIPITATION CHARACTERISTICS

From the starting and ending dates (Fig. 4), the average wet season length is calculated and presented in Fig. 9. Throughout most of Mexico and New Mexico

the season lasts about 100 days, but it is shorter in Arizona and longer in southern Mexico. The average wet-season rain rate is shown in Fig. 10a. This quantity is computed at each grid point by summing wet season rainfall for all years and dividing by the total number of wet season days. The pattern matches that of annual precipitation quite well (Fig. 1); that is, large annual totals correspond to large wet-season rain rates. The correspondence is particularly good in the monsoon core region. The tongue of maximum rain rate extends westward through northwestern Mexico, reaching the U.S. border at central Arizona. As with annual total precipitation (Fig. 1), it is difficult to see evidence of the monsoon in most of Arizona and New Mexico. The monsoon signal in New Mexico emerges only in maps of the percent of annual precipitation during the wet season (not shown). The wet-season rain rate exceeds 8 mm day^{-1} in southern Mexico, is between 6 and 7 mm day^{-1} over a large area of the monsoon region, and decreases to about 3 mm day^{-1} in the vicinity of the Arizona–Sonora, Mexico, border. By way of comparison, the wet season rate is about 10 mm day^{-1} in the central Amazon basin of South America (not shown).

Figure 10b shows the average wet-day rain rate during the wet season. The rate was calculated from the individual stations within a particular grid point by summing the rainfall at each station for each year's local wet season (gridpoint onset to end) and dividing by the number of wet days at that station. The gridpoint average of that value is then averaged again over all years. The wet-day rain rate appears to be related to the distance from the coast: the largest rates are found along the Gulf of Mexico coast, exceeding 15 mm day^{-1} over most of the coastal plain. The lowest rates occur in the interior of the Mexican Plateau with a general decrease toward the north. For the core of the monsoon, this finding was also obtained by Gochis et al. (2007a), who analyzed data from a research-quality rain gauge observing network in northwest Mexico.

The largest wet day frequency (Fig. 10c), again calculated from individual stations over the yearly varying gridpoint wet season, coincides almost exactly with the core of the monsoon and with the spine of the Sierra

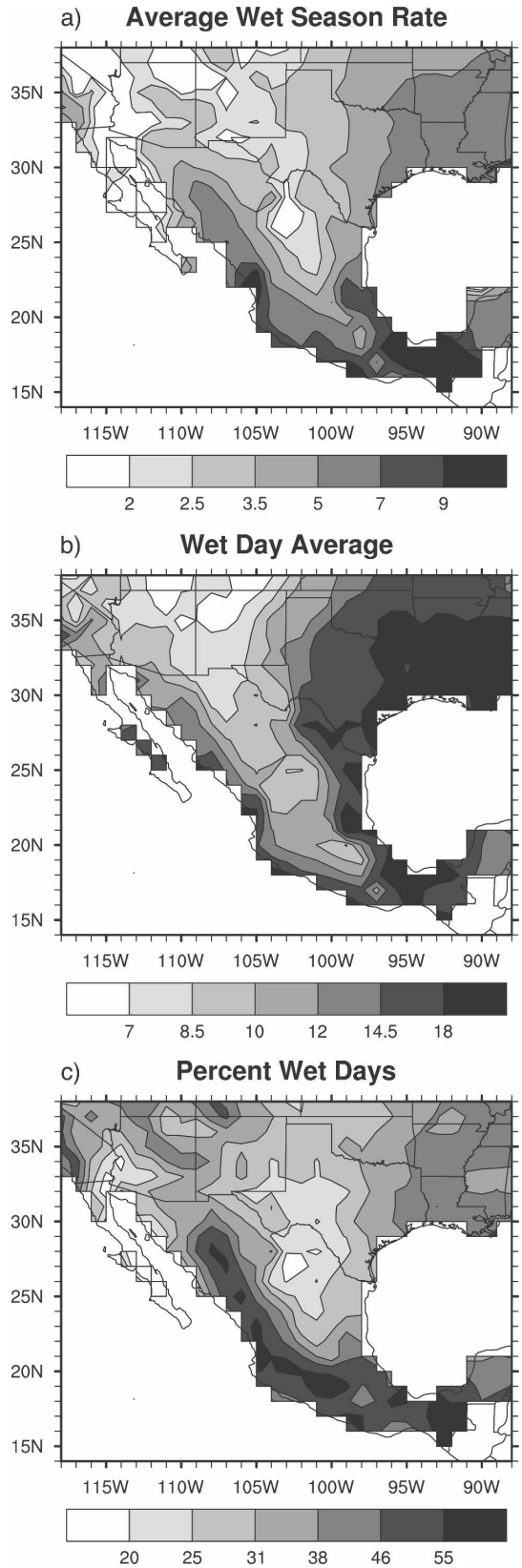

→

FIG. 10. (a) Climatological wet-season rain rate (mm) calculated at each grid point as average of rate for each interannually varying wet season. (b) Wet season wet-day average (mm day^{-1}) calculated first at each station within capture radius of grid point as total wet season (determined each year from gridded fields) precipitation divided by number of days with precipitation, and then averaged over all stations for all years. (c) As in (b), but for wet-day frequency (%).

Madre: it is thus not related to coastal proximity. A similar pattern has been reported by Gochis et al. (2004). Figure 10c indicates that rain occurs on at least 50% of the days during the wet season until about 30°N, north of which the percent of wet days decreases to around 35% at the U.S. border. In the Arizona–New Mexico region, the frequency is largest near the border between those states and decreases to the east and west.

Thus, from a spatial perspective, the maximum in the wet-season rain rate associated with the monsoon appears to be due to a combination of increased incidence of wet days, distinctly related to topography, and a gradient in the wet-day rain rate toward the coast. The result is a maximum in wet season precipitation that is located slightly to the west of the maximum elevation of the Sierra Madre. This westward shift of maximum rainfall relative to topography was also noted by Gochis et al. (2004), who speculated, consistent with our findings, that the quantity of seasonal precipitation is related to distance from the coast.

b. *Interannual variability*

1) DIAGNOSTIC RELATIONSHIPS

As mentioned in the introduction, we expect a large part of summer rainfall interannual variability (especially in the core of the monsoon region where a large fraction of the annual total falls during the wet season) to be attributable to variations in the wet season length and the wet-season rain rate. Figure 11a, which shows the relationship between these two quantities, expressed as the mutual variance explained by one another (i.e., the square of the correlation), indicates that they are largely independent of each other over the area dominated by the monsoon, except in parts of Arizona and New Mexico. In the domain considered here, the sign of the correlation between the two is weakly negative everywhere.

The interannual variance of June–October precipitation explained by the length and rain rate of the wet season is presented in Figs. 11b and 11c (the corresponding correlations are positive everywhere, as would be expected). In the core area, the variance accounted for by the wet season length is largest in the north, with more than 35% explained variance over

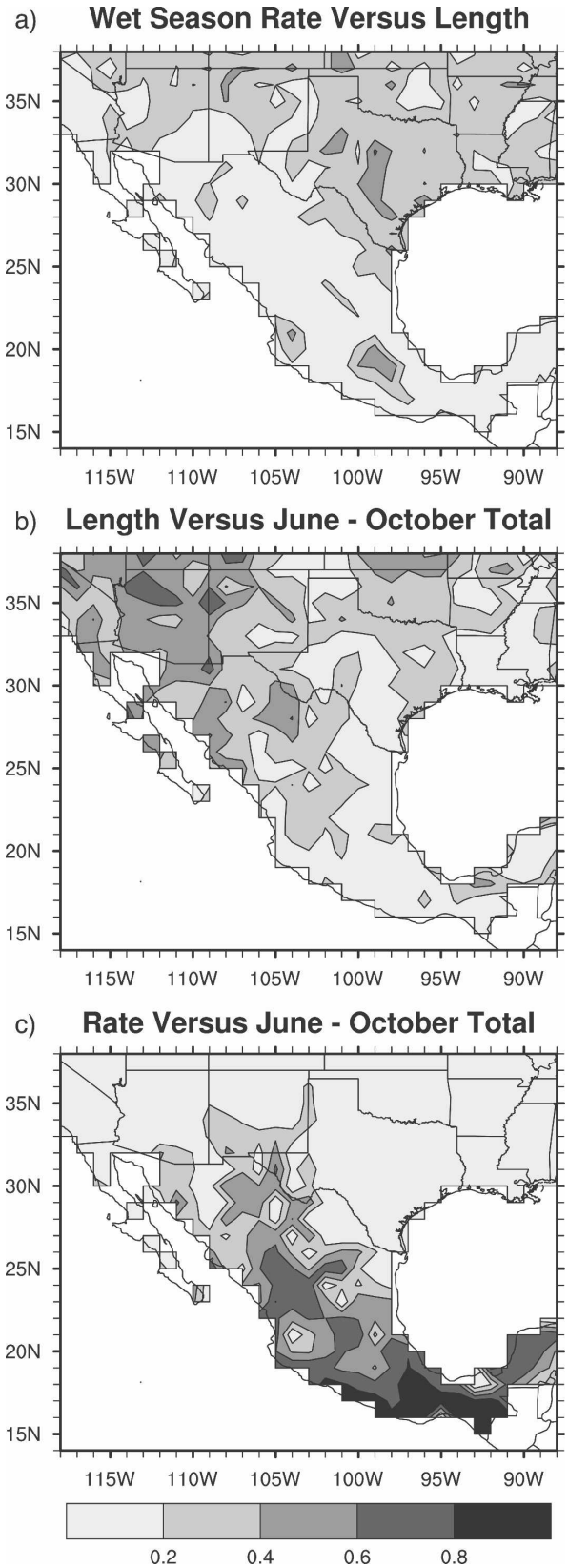

→

FIG. 11. Interannual variance mutually explained at each grid point by (a) wet-season rain rate and wet season length; (b) wet season length and June–October precipitation; and (c) wet-season rain rate and June–October precipitation.

Arizona, and decreases to less than 20% over most of Mexico (Fig. 11b). Variations in the wet-season rain rate, on the other hand, account for a large portion of the interannual variability in summer precipitation, mainly in Mexico (Fig. 11c), and their importance increases toward the south (although in areas in which the wet season starts before 1 June, for example, south of about 20°N, the plot is somewhat misleading). The decreasing importance of wet season length and increasing importance of rain rate toward the south is consistent with the fact that the monsoon length increases toward the south (Fig. 9). As the wet season becomes longer, variations in length result in less of a fractional change in total precipitation but variations in the mean rain rate can impact over a longer period (provided the year-to-year changes in the season length do not systematically vary with latitude).

The wet-season rain rate can be separated into a product of contributions from the wet-day frequency and the wet-day rain rate, whose climatologies were shown in Fig. 10 (recall that, at each grid point, the wet-day rate and frequency are gridpoint averages over all stations within the capture radius of that grid point). Figure 12a shows variations of these two quantities to be largely unrelated. Figures 12b and 12c reveal similar contributions to the wet-season rain rate variability from changes in wet-day frequency and rain rate, although the former is relatively constant in space, while the latter decreases to the northwest.

To summarize, changes in season length dominate the variability of total summer precipitation in the northern monsoon region, while the wet-season rate becomes increasingly important toward the south. In the south, variability in both the wet-day frequency and rain rate, themselves nearly independent, contribute substantially to the warm-season precipitation variability.

2) Relationships with sea surface temperatures

Summer seasonal precipitation totals in some areas of North America are known to be modestly related to SST anomalies in both the tropics and the extratropics. For example, HCD99 found that, in southwestern Mexico, dry monsoons tend to occur during El Niño and wet monsoons during La Niña, although they noted

→

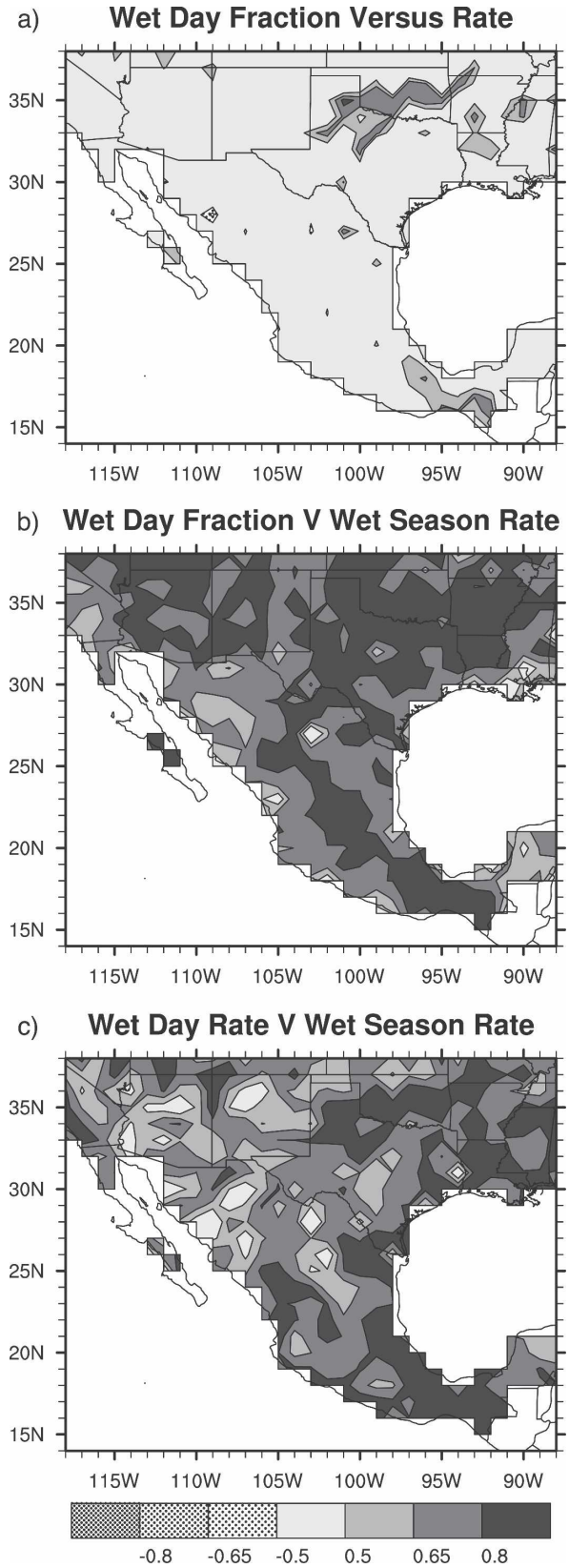

FIG. 12. (a) Interannual correlation between wet season wet-day fraction (frequency) and wet-day rain rate. (b) As in (a), but for correlation between wet-day fraction and wet season rate. (c) As in (a), but for correlation between wet-day rain rate and wet-season rain rate.

that other "factors" were also likely to be important. Englehart and Douglas (2006) found that, in northwestern Mexico, a short wet season with a late start occurs with El Niño. They noted that variations in intensity, however, are more closely related to variations in seasonal totals than to variations in wet season length. Castro et al. (2001) found that, in the southwestern United States, the most consistent impact of the ocean on monsoon precipitation occurs when El Niño (La Niña) conditions in the tropical Pacific coincide with warm (cold) SST anomalies in the eastern North Pacific and cold (warm) SST anomalies in the central North Pacific, which results in decreased (increased) precipitation. Brito-Castillo et al. (2003) found El Niño events to be associated with reduced rainfall in the Gulf of California watershed. Given the known associations between SST and monsoon precipitation, it is of interest to determine the nature of that influence, for instance, whether it operates through changes in the wet season length or rain rate.

As a means of identifying linear relationships between SSTs and North American summer rainfall, a singular value decomposition (SVD; see Wallace et al. 1992) was performed on the June–August (JJA) U.S.–Mexican precipitation dataset and adjacent SST field (i.e., over the region 10°S–40°N, 120°E–360°). The leading SVD mode of SST and precipitation (not shown) explains 51% of the total squared covariance between the two fields, with the SST pattern being most pronounced over the Pacific. To check the physical validity of this SVD mode, an empirical orthogonal function decomposition, based on the covariance matrix, was also performed on Pacific SST data only (from 10°S to 40°N). The leading principal component explains 40% of the variance (in that SST domain) and is correlated with the SST time series of the leading SVD mode of hemispheric SST and rainfall at 0.99. Thus this dominant EOF of Pacific SST is also the global SST pattern most closely coupled with U.S.–Mexican rainfall. This correspondence allows us to proceed with the analysis by simply using the time series of this leading EOF as representing large-scale interannual SST variability that is most relevant for monsoon rainfall variability. This leading EOF, presented in Fig. 13a, displays maximum amplitude over the tropical eastern Pacific and is clearly associated with ENSO. Note also the weaker anomalies of the same sign along the Pacific Mexican coast.

The correlation between the time series of the leading EOF of SST and JJA rainfall (Fig. 13b) reveals negative correlations over a broad area of central and southwestern Mexico. Note that the shading starts at ±0.3, which is not statistically significant at the 95% level (using a two-sided t test), but is intended to illustrate that the correlations in southern Mexico are all of the same sign. This pattern is consistent with the findings of HCD99 and Gochis et al. (2007a), who showed deficits of rainfall and streamflow, respectively, in southwest Mexico associated with El Niño. Note also the weak correlations over northern Mexico and the United States.

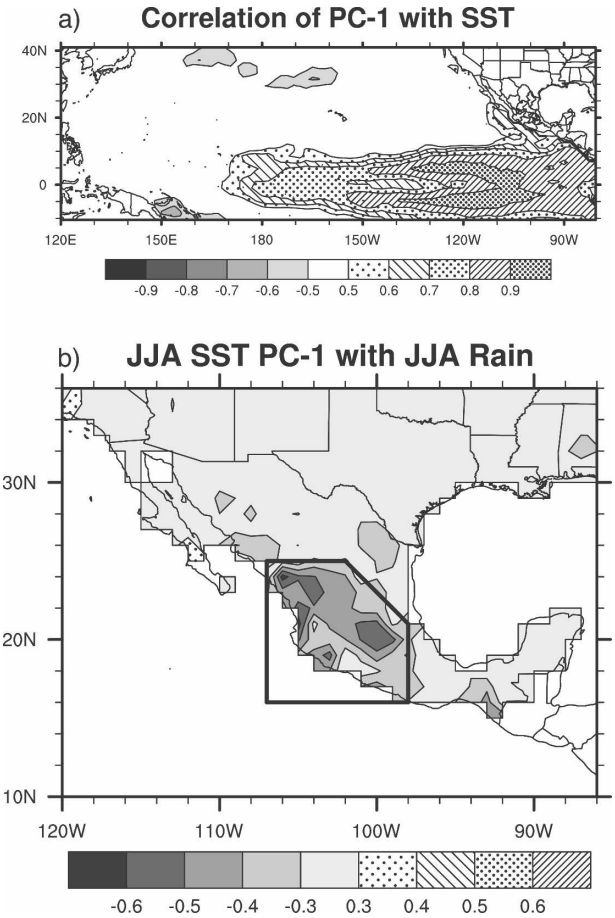

FIG. 13. (a) Correlation between principal component of leading EOF of interannual June–August SST for the period 1966–2000 over domain shown and SST at each grid point. (b) Correlation between the same principal component and June–August precipitation. Box shows averaging area used to construct the precipitation indices correlated with SST in Fig. 14.

An index of Mexican monsoon precipitation is then constructed by averaging JJA precipitation over the grid points that exhibit the largest negative correlations with the leading EOF of SST (see the box in Fig. 13b), that is, an area encompassing most of central and southwest Mexico. As expected, the pattern that emerges when this index is correlated with SST reveals a negative association between Mexican precipitation and tropical Pacific SSTs (Fig. 14a). The correlation pat-

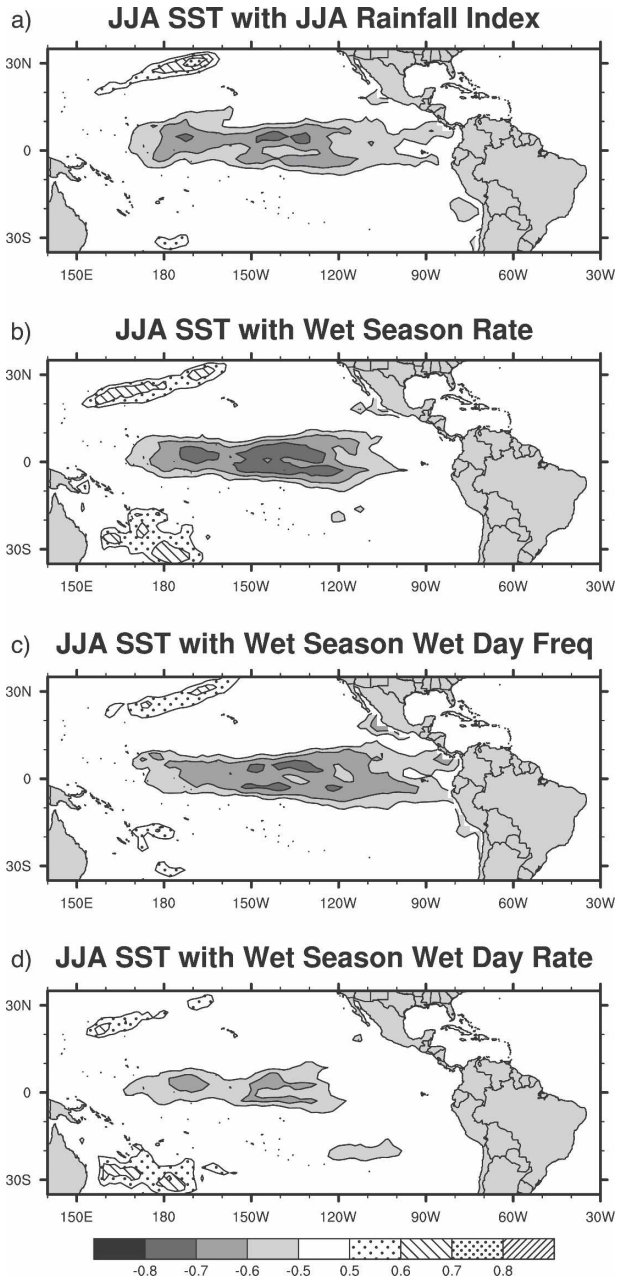

FIG. 14. (a) Interannual correlation between June–August SST and index of total June–August precipitation for average of grid points within box shown in Fig. 13b. (b) As in (a), but index is average gridpoint wet season rate. (c) As in (a), but index is interannual wet-day frequency averaged over individual stations within box. (d) As in (c), but index is wet-day rain rate.

tern, however, is shifted to the west relative to the SST EOF pattern (Fig. 13b), which indicates that Mexican rainfall is more sensitive to SST variations in the central than in the eastern tropical Pacific.

The correlation between the wet-season rain rate (recall section 3a), averaged over the same grid points, and SST (Fig. 14b) is somewhat stronger than that between the JJA total and SST (Fig. 14a). This is presumably due to the lack of relationship between season length (averaged over the box) and SST (not shown) so that random variations in season length weaken the SST–wet season precipitation correlation.

The correlations between SST and wet-day frequency and wet-day rain rate, computed as before and averaged over the box in Fig. 13b (Figs. 14c,d), suggest that the modulation of Mexican rainfall by warm tropical Pacific SSTs occurs through a decrease in the frequency of rainy days rather than through a decrease in the amount of rainfall on wet days.

4. Summary

The climatology and interannual variability of summertime North American precipitation is examined using daily data from rain gauges. As shown in earlier studies, there is a maximum in the total annual amount, relative to other longitudes, extending along the Sierra Madre Occidental and into the southwestern United States, that results primarily from summer rainfall.

Onset and end of the wet season are determined at each grid point for each year by finding those periods during which rainfall exceeds its annually averaged daily rate. Averaging these dates over the period of record reveals that the wet season begins in May throughout most of eastern and southern Mexico. In the region broadly corresponding to the Sierra Madre Occidental, the wet season begins in late May in the south and reaches Arizona in late June. In the core of the monsoon region, this evolution is qualitatively consistent with the progression shown by HCD99.

In southern and eastern Mexico onset appears to be triggered by changes in vertical velocity, since the stability is low long before onset. In the northern portion of the domain, onset seems to be related to a decrease in stability, since vertical velocity is upward for days before the initiation of convection.

The wet season withdraws from northwest to southeast over a period of about three weeks starting around mid-September, although this date is undoubtedly influenced by the presence or absence of tropical storms. The length of the monsoon season ranges from less than two months in northwestern Arizona to more than four in southern Mexico.

The average wet-season rain rate is largest and relatively uniform along the mountains in southern and central Mexico. It then decreases rapidly to about half that value in northwestern Mexico and the southwestern United States The wet-day rain rate during the wet season roughly decreases with distance from the coast,

but the wet-day frequency is greatest along the spine of the Sierra Madre. The maximum in seasonal (and annual) rainfall is therefore a combination of the wet-day frequency and wet-day rain rate and is maximum slightly west of the spine of the mountains, consistent with the results of Gochis et al. (2004, 2007b).

The rain rate during the wet season is more strongly affected by variations in the wet-day frequency than by variations in the amount of rain per event, especially in northwestern Mexico and the southwestern United States. The wet-day rates and the wet-day frequencies are largely unrelated.

The leading EOF of Pacific JJA SSTs is correlated with JJA rainfall in southern Mexico. Rainfall tends to be reduced when equatorial Pacific SSTs are anomalously warm, consistent with previous studies. Further analysis using indices of precipitation statistics averaged over southern Mexico reveal that the modulation of rainfall by tropical SSTs occurs mostly through variations in the wet-day frequency and, to a lesser extent, through variations in the wet-day rate, but not through variations in the wet season length.

The inverse relationship between the wet-day rate and distance from the coast suggests that water vapor content (i.e., precipitable water) tends to determine the rainfall amount per event and that the proximate seas are the source of that vapor. It is therefore somewhat surprising that there is no obvious interannual relationship between adjacent SSTs and the wet-day rate. Thus interannual variations in wet-day rate (and, presumably, humidity) appear to be more related to changes in the atmospheric circulation than in the local evaporation. On the other hand, the 100-yr period of record examined by Hu and Feng (2004) suggests there have been epochs for which local land processes were important. Further work is required to assess the role of the various processes associated with both land surface feedbacks and SST forcing in determining monsoon variability at different time scales.

Acknowledgments. We wish to thank the Servicio Meteorológico Nacional de México for generously providing station precipitation and temperature observations for Mexico. U.S. precipitation data are from the U.S. Cooperative Observing Network and were obtained from the National Climatic Data Center. We wish to thank NOAA/CPPA for partially supporting this research.

REFERENCES

Adams, D. K., and A. C. Comrie, 1997: The North American monsoon. *Bull. Amer. Meteor. Soc.,* **78,** 2197–2213.

Barlow, M., S. Nigam, and E. H. Berbery, 1998: Evolution of the North American monsoon system. *J. Climate,* **11,** 2238–2257.

Brito-Castillo, L., A. V. Douglas, A. Leyva-Contreras, and D. Lluch-Belda, 2003: The effect of large-scale circulation on precipitation and streamflow in the Gulf of California continental watershed. *Int. J. Climatol.,* **23,** 751–768.

Carleton, A. M., D. A. Carpenter, and P. J. Weser, 1990: Mechanisms of interannual variability of the southwest United States summer rainfall maximum. *J. Climate,* **3,** 999–1015.

Castro, C. L., T. B. McKee, and R. A. Pielke Sr., 2001: The relationship of the North American monsoon to tropical and North Pacific sea surface temperatures as revealed by observational analyses. *J. Climate,* **14,** 4449–4473.

Douglas, A. V., and P. J. Englehart, 1995: An analysis of the starting date for the summer monsoon in western Mexico and southeast Arizona. *Proc. 20th Annual Climate Diagnostics Workshop,* Seattle, WA, Climate Prediction Center, 207–211.

——, and ——, 1996: Variability of the summer monsoon in Mexico and relationships with drought in the United States. *Proc. 21st Annual Climate Diagnostics Workshop,* Huntsville, AL, Climate Prediction Center, 296–299.

Douglas, M. W., R. Maddox, K. Howard, and S. Reyes, 1993: The Mexican monsoon. *J. Climate,* **6,** 1665–1677.

Englehart, P. J., and A. V. Douglas, 2001: The role of eastern North Pacific tropical storms in the rainfall climatology of western Mexico. *Int. J. Climatol.,* **21,** 1357–1370.

——, and ——, 2006: Defining intraseasonal rainfall variability within the North American monsoon. *J. Climate,* **19,** 4243–4253.

Gochis, D. J., A. Jimenez, C. J. Watts, J. Garatuza-Payan, and W. J. Shuttleworth, 2004: Analysis of 2002 and 2003 warm-season precipitation from the North American Monsoon Experiment Event Rain Gauge Network. *Mon. Wea. Rev.,* **132,** 2938–2953.

——, L. Brito-Castillo, and W. J. Shuttleworth, 2007a: Correlations between sea-surface temperatures and warm season streamflow in northwest Mexico. *Int. J. Climatol.,* **27,** 883–901.

——, C. J. Watts, J. Garatuza-Payan, and J. Cesar-Rodriguez, 2007b: Spatial and temporal patterns of precipitation intensity as observed by the NAME Event Rain Gauge Network from 2002 to 2004. *J. Climate,* **20,** 1734–1750.

Gutzler, D. S., 2000: Covariability of spring snowpack and summer rainfall across the southwest United States. *J. Climate,* **13,** 4018–4027.

——, 2004: An index of interannual precipitation variability in the core of the North American monsoon region. *J. Climate,* **17,** 4473–4480.

——, and Coauthors, 2005: The North American monsoon model assessment project: Integrating numerical modeling into a field-based process study. *Bull. Amer. Meteor. Soc.,* **86,** 1423–1429.

Higgins, R. W., and W. Shi, 2000: Dominant factors responsible for interannual variability of the summer monsoon in the southwestern United States. *J. Climate,* **13,** 759–776.

——, Y. Yao, and X. L. Wang, 1997: Influence of the North American monsoon system on the U.S. summer precipitation regime. *J. Climate,* **10,** 2600–2622.

——, K. C. Mo, and Y. Yao, 1998: Interannual variability of the U.S. summer precipitation regime with emphasis on the southwestern monsoon. *J. Climate,* **11,** 2582–2606.

——, Y. Chen, and A. V. Douglas, 1999: Interannual variability of the North American warm season precipitation regime. *J. Climate,* **12,** 653–680.

Hu, Q., and S. Feng, 2002: Interannual rainfall variations in the

North American summer monsoon region: 1900–98. *J. Climate,* **15,** 1189–1202.

——, and ——, 2004: Why has the land memory changed? *J. Climate,* **17,** 3236–3243.

Kalnay, E., and Coauthors, 1996: The NCEP/NCAR 40-Year Reanalysis Project. *Bull. Amer. Meteor. Soc.,* **77,** 437–471.

Liebmann, B., and D. Allured, 2005: Daily precipitation grids for South America. *Bull. Amer. Meteor. Soc.,* **86,** 1567–1570.

——, and Coauthors, 2004: An observed trend in central South American precipitation. *J. Climate,* **17,** 4357–4367.

Magaña, V., J. A. Amador, and S. Medina, 1999: The midsummer drought over Mexico and Central America. *J. Climate,* **12,** 1577–1588.

Mapes, B. E., P. Liu, and N. Buenning, 2005: Indian monsoon onset and the Americas midsummer drought: Out-of-equilibrium responses to smooth seasonal forcing. *J. Climate,* **18,** 1109–1115.

Mechoso, C. R., A. W. Robertson, C. F. Ropelewski, and A. M. Grimm, 2005: Part B: Regional monsoon topics. The American monsoon systems: An introduction. WMO Tech. Doc. 1266 (TMRP Rep. 70), World Meteorological Organization, 197–206.

Mesinger, F., and Coauthors, 2006: North American Regional Reanalysis. *Bull. Amer. Meteor. Soc.,* **87,** 343–360.

Portig, W. H., 1961: Some climatological data of Salvador, Central America. *Weather,* **16,** 103–112.

Ropelewski, C. F., D. S. Gutzler, R. W. Higgins, and C. R. Mechoso, 2005: The North American monsoon system. The Global Monsoon System: Research and Forecasts. WMO Tech Doc. WMO TD-1266, Tropical Meteorology Research Program Rep. 70, 207–218.

Vera, C., and Coauthors, 2006: Toward a unified view of the American monsoon systems. *J. Climate,* **19,** 4977–5000.

Wallace, J. M., C. Smith, and C. S. Bretherton, 1992: Singular value decomposition of wintertime sea surface temperature and 500-mb height anomalies. *J. Climate,* **5,** 561–576.

Yu, B., and J. M. Wallace, 2000: The principal mode of interannual variability of the North American monsoon system. *J. Climate,* **13,** 2794–2800.